STUDY ON PHOTOCATALYTIC PROPERTIES OF BISMUTH OXYCHLORIDE CATALYSTS

Aye Aye Lwin[1], Aung Khaing[2]*, Aung Than Htwe [2]

Abstract

Well-crystallized flake-like bismuth oxychloride nanoparticles (BiOCl NPs) were successfully synthesized by a solvothermal process using bismuth(III) nitrate pentahydrate ($Bi(NO_3)_3.5H_2O$) and potassium chloride (KCl) with various ratios of ethanol and distilled water (10:90, 25:75, 50:50, 75:25, and 90:10 v/v). The synthesized BiOCl NPs were characterized by using XRD, SEM, UV-visible, FT IR and TG-DTA analysis. Degradation of Rhodamine B and Eriochrome Black T in aqueous media was estimated spectrophotometrically in the visible range at 553 and 545 nm, respectively. Among them, BiOCl-4 showed the highest photodegradation performance under UV light exposure due to the formation of nanosheets. The mechanism of synthesized BiOCl-4 is evaluated by conduction band and valence band values. So, the synthesized BiOCl NPs can be used as photocatalysts in the photodegradation of aqueous organic dyes.

Keywords: BiOCl NPs, solvothermal process, photodegradation, organic dyes

Introduction

Nanoparticles (NPs) are assigned as nanoentries whose size ranges from 1 to 100 nm. According to their smaller size, nanoparticles present a much higher specific surface area because the total surface area of a particle is inversely proportional to its diameter. Nanoparticles have promising potential for use in various applications due to their unusual characteristics compared to bulk materials. Nanotechnology is used in the creation, investigation, and application of new types of materials, called nanomaterials. Nanomaterials are used in industrial chemistry, agriculture engineering, pharmaceutics, and medicine (Dudchenko *et al.*, 2022). Bismuth oxychloride nanoparticles were used to degrade pollutants such as pesticides, antibiotics, heavy metal ions, and microorganisms. BiOCl nanoparticles have a unique layered structure, electronic properties, optical properties, good photocatalytic activity, and stability (Wang *et al*., 2022).

Bismuth oxyhalides, BiOX (X= Cl, Br, I), have been found useful in various applications because of their optical properties, such as as photocatalysts. BiOX belongs to the V-VI-VII groups of compound semiconductors with a tetragonal system. The structure of BiOX is known to have a layered structure that is constructed by combining the halide ion layer and the bismuth oxygen layer (Tripathi *et al*., 2015). It has exhibited wide applications as a pigment in the cosmetic industry, a photocatalyst in degrading organic pollutants, and for optoelectronic and photovoltaic devices, e.g., light-emitting diodes, lasers, and solar cells (Cao *et al.*, 2009). Bismuth oxychloride (BiOCl), with a band gap energy of 3.5 eV, has been used as a catalyst for the oxidative cracking of hydrocarbons and photoluminescent materials. BiOCl nanoparticles can be an efficient photocatalyst for decomposing methyl orange under UV light.

Materials and Methods

Bismuth (III) nitrate pentahydrate, $Bi(NO_3)_3.5H_2O$, potassium chloride (KCl), ethanol, (EtOH) and ammonia (NH_3) were of analytical grade and used directly without further purification. Distilled water was used throughout all the experiments.

[1] Department of Chemistry, University of Yangon, Myanmar
[2] Department of Chemistry, University of Yangon, Myanmar

Synthesis of BiOCl NPs

To synthesize the first sample of BiOCl, 100 mL of bismuth nitrate solution was prepared by dissolving 4 g of $Bi(NO_3)_3.5H_2O$ in the first solvent, i.e., ethanol: water: (10:90), and 50 mL of KCl solution was prepared by dissolving 0.75 g of KCl in (10:90) ($EtOH:H_2O$). $Bi(NO_3)_3.5H_2O$ solution was taken in a conical flask and placed on the magnetic stirrer. KCl solution was allowed to flow into the Bi $(NO_3)_3.5H_2O$ solution in the conical flask at 2.5 mL min^{-1} with continuous stirring. After the complete addition of 50 mL KCl solution, 5 mL of 25 % NH_3 solution was added to maintain the pH of the mixture at 2, and stirring was further continued for 10 h to ensure the completion of the reaction, i.e., the precipitation of bismuth oxychloride. The resulting precipitates were collected by filtration and washed several times with distilled water for complete removal of undesirable water-soluble products. Solid compound so obtained was subsequently dried at 80 ˚C for 24 h in an oven. The above procedure was repeated to synthesize four other samples of BiOCl using the solvent composition ethanol: water as 25:75, 50:50, 75:25, and 90:10 (v/v).

Characterization

The crystal phases of the BiOCl NPs were analyzed by using an X-ray powder diffractometer (XRD). The surface morphology of synthesized samples was observed with scanning electron microscope (SEM) (EVO-18, Probe Micro Analyzer, Germany). Fourier transform infrared spectroscopy (FT IR) was measured for functional group estimation using (FT IR-8400, PerkinElmer GX system; USA). The wavelengths of maximum absorption of synthesized BiOCl NPs were determined by UV-Vis spectroscopy (UV-mini 1240). Finally, the weight loss of BiOCl NPs was measured by using TG-DTA.

Photocatalytic Activity

The photocatalytic efficiency of BiOCl NPs was assessed with a degradation of Rhodamine B (RhB) and Eriochrome Black T (EBT) using Ultraviolet light irradiation. In a process, 30 mg of BiOCl NPs were added to 50 mL of solution containing 200 mgL^{-1} RhB and EBT dye concentration. The solution was stirred for 30 min in the dark. After that, the solution was exposed to UV light. The 3 mL each of RhB and EBT dye samples were taken at 3 min intervals and instantly centrifuged at 1000 rpm for 2 min to isolate the photocatalyst particles. Finally, absorbance of the dye sample was noted at UV visible spectrophotometer at 553 nm (RhB) and 545 nm (EBT) wavelengths.

Results and Discussion

Structure of BiOCl NPs

X-ray power diffraction peaks were analyzed to investigate the phase structure of synthesized BiOCl NPs, as shown in Figure 1. The diffraction peaks of synthesized samples appear at 2θ values, which match with (hkl) values according to entry card no. (96-450-9950) corresponding to the tetragonal system, respectively (Sharma *et al*., 2015). Four characteristic peaks of BiOCl were observed around 2θ of 11.98˚, 25.81˚, 32.48˚, and 34.50˚ corresponding to Miller indices of (001), (101), (110), and (012) planes, respectively, which are in good agreement with the planes of BiOCl obtained from the entry card number. XRD data confirmed the formation of a crystalline tetragonal phase of BiOCl NPs . Using Scherrer's equation, the average crystallite sizes were determined to be 19.98 nm for BiOCl-1, 28.86 nm for BiOCl-2, 20.24 nm for BiOCl-3, 32.23 nm for BiOCl-4, and 21.24 nm for BiOCl-5.

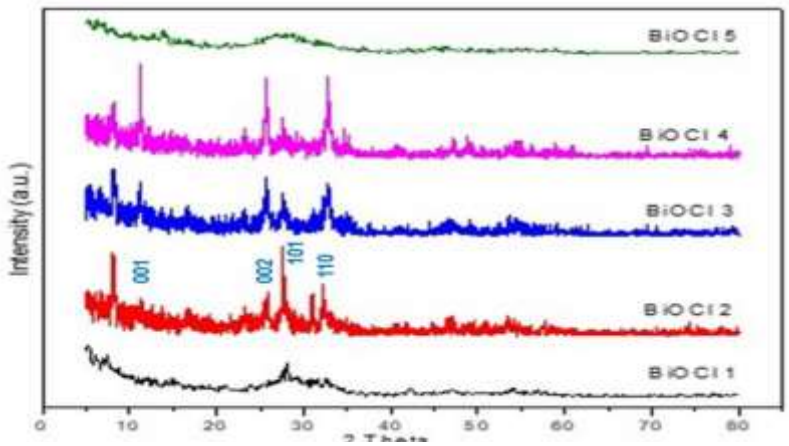

Figure 1. XRD patterns of synthesized BiOCl

FT IR Spectroscopy

The results of the FT IR spectra analysis of the synthesized BiOCl-1, BiOCl-2, BiOCl-3, BiOCl-4, and BiOCl-5 samples are shown in Figure 2. As shown in Figures 2(a to e), the absorption bands of all BiOCl samples were observed in the range 1400-1600 cm^{-1}, which can be assigned to the skeletal stretching vibration mode of Bi-Cl. The characteristic peak of 1155 cm^{-1} can be assigned to the stretching vibration mode of Bi-Cl, and 512 cm^{-1} can be assigned to the vibration mode of Bi-O (Seddigi *et al*., 2017).

UV-Vis Absorption Spectra

The UV-Vis spectra (Figure 3) of BiOCl NPs show absorption maxima between 210 and 275 nm due to the n to π* electronic transition of synthesized BiOCl NPs. The other peak of 254 nm was due to the ethanol solvent effect (Silverstein and Webster, 1998; Schwartz, 1965).

Morphology of BiOCl NPs

Figure 4 shows the SEM images of synthesized BiOCl-1 to 5 NPs in different solvents by the solvothermal method, respectively. These images were obtained at a 7 kV accelerating voltage with 20,00 times magnification. The synthesized samples consisted of a large number of flake- like nanosheets. According to SEM images, the porosity of BiOCl-1 has the highest value compared to other samples.

But BiOCl-4 has the highest flake-like nanosheet and cluster of aggregation because it depends on the ethanol- solvent ratio (75:25). BiOCl-1 is bulky and clustered in its amorphous form. BiOCl-2 has a bulky shape with aggregation. BiOCl-3 belongs to a flake-like aggregation cluster. BiOCl-5 has a rod-like shape and a cluster of nanorod.

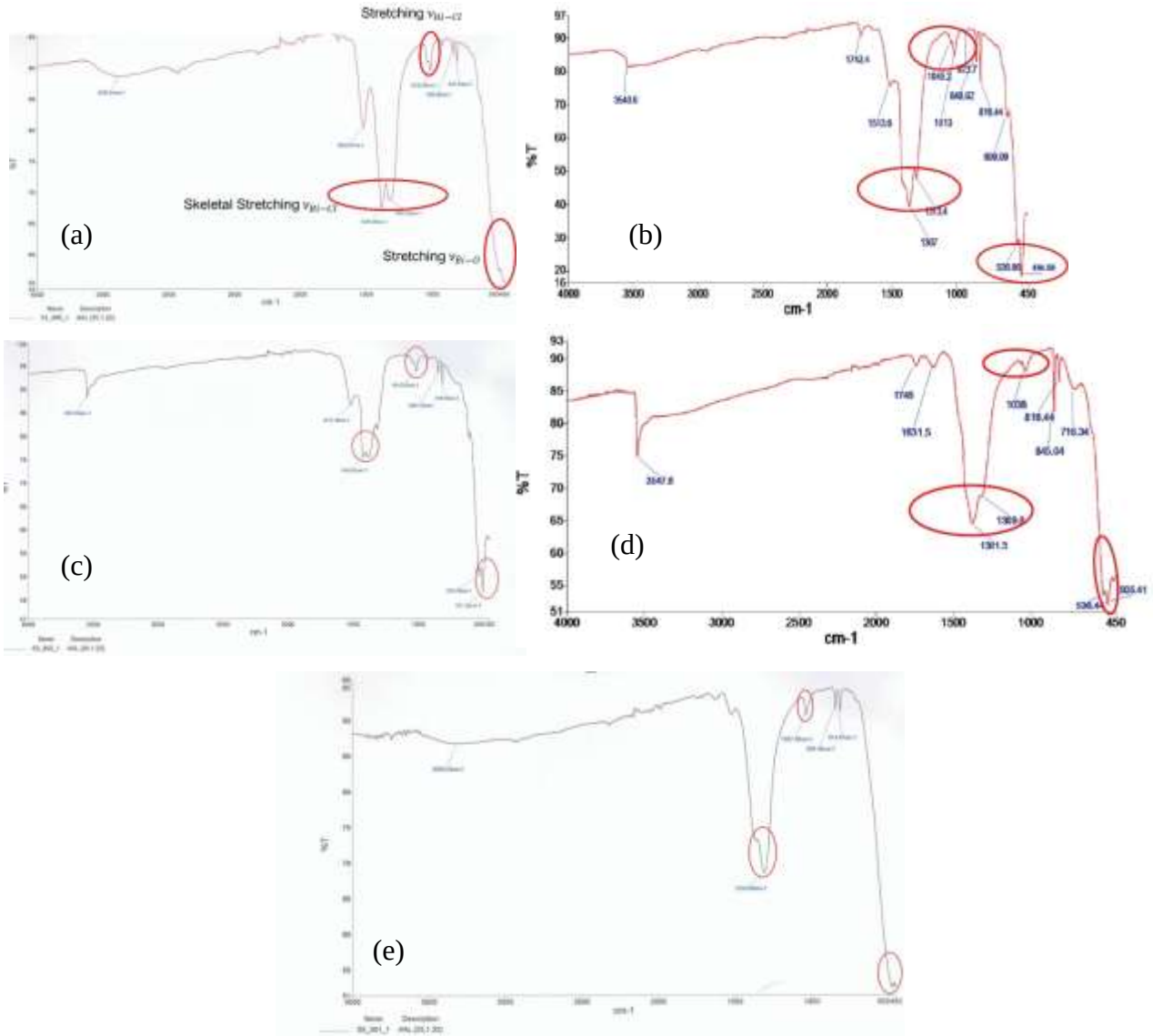

Figure 2. FT IR spectra of (a) BiOCl-1, (b) BiOCl-2, (c) BiOCl-3, (d) BiOCl-4, and (e) BiOCl-5

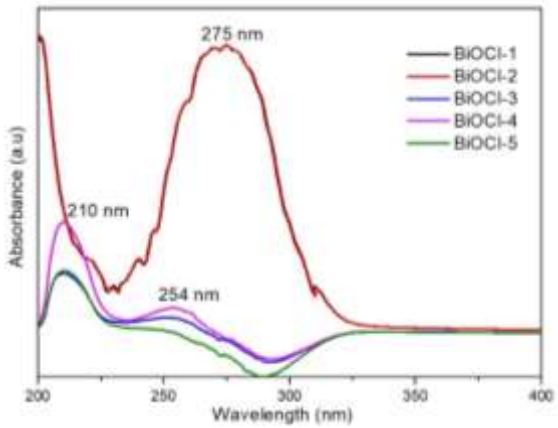

Figure 3. UV-vis spectra of synthesized BiOCl NPs

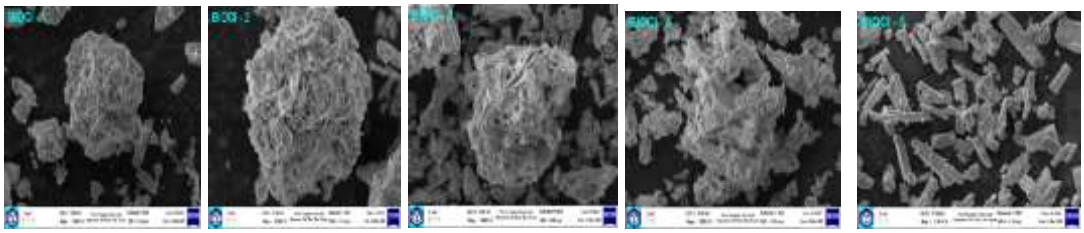

Figure 4. SEM images of BiOCl NPs

Optical Properties of Synthesized BiOCl NPs

As the ethanol solvent increases to 75 %, the absorption wavelength of BiOCl-4 increases to 254 nm. The band gap energy of semiconductor can be calculated approximately by using the Tauc Plot, $(\alpha h\nu)^2$ vs $h\nu$, where α, h, and ν are the absorption coefficient, Planck's constant, and light frequency, respectively. As can be seen in Figure 5, E_g values of BiOCl NPs gradually decrease with increasing ratio of the ethanol to 90 %, changing from 4.06 to 3.6 eV as determined from a plot of $(\alpha h\nu)^2$ vs $h\nu$. According to the literature, the common band gap value of BiOCl is 3.2 eV. In this work, the band gap value of BiOCl NPs reduced from 4.06 eV to 3.7 eV. It can be compared with the literature value of 3.2 eV; the band gap value of synthesized BiOCl-4 is in close agreement with the earlier reports (Tripathi *et al*., 2015). From these results, it can be deduced that all the synthesized BiOCl NPs 1 to 5 have suitable band gaps to be activated by ultraviolet light for photocatalytic decomposition of organic and inorganic pollutants.

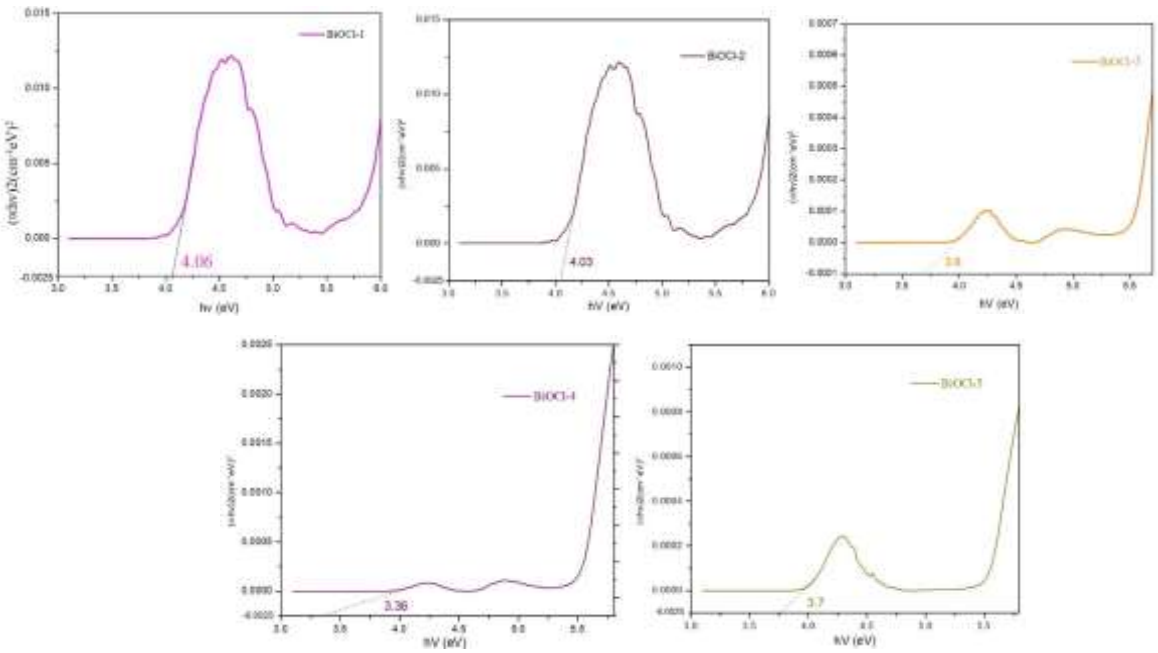

Figure 5. Tauc plots of BiOCl NPs 1 to 5

Thermogravimetric analysis

Thermogravimetric (TG) and differential thermal analysis (DTA) thermograms of synthesized BiOCl NPs were carried out at room temperature up to 80 ºC. TG-DTA thermogram profiles of the BiOCl NPs are shown in Figure 6(a to e). All of the BiOCl NPs cause weight loss in three stages. The first stage range is about 38 ºC to 88 ºC with weight loss of 0.93 % for BiOCl-1, 1.34 % for BiOCl-2, 0.41 % for BiOCl-3, 0.49 % for BiOCl-4, and 1.69 % for BiOCl-5. There is a loss of surface water.

In the second stage of the temperature range between 88 ºC and 216 ºC the weight losses were observed to be 10.30 % for BiOCl-1, 6.01 % for BiOCl-2, 3.48 % for BiOCl-3, 2.15 % for BiOCl-4, and 2.38 % for BiOCl-5. This is due to the evaporation of water and the surface of NO_3 group adsorbed on the BiOCl NPs. The third stage is the weight loss of 7.81 % for BiOCl-1, 3.00 % for BiOCl-2, 2.99 % for BiOCl-3, 2.54 % for BiOCl-4, and 3.90 % for BiOCl-5 which were observed to take place within the temperature range of 218 ºC to 329 ºC. At this stage, the weight loss may be due to complete combustion of residue at an exothermic temperature of about 314 ºC.

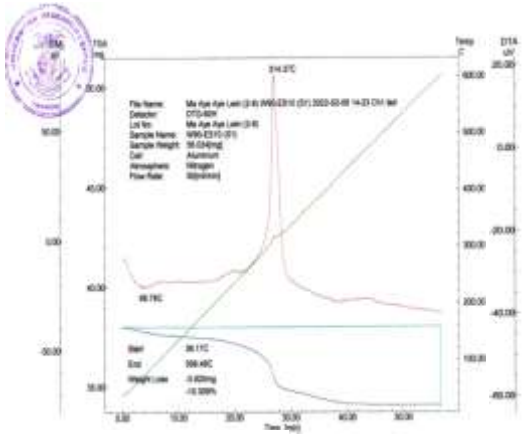

(a) BiOCl-1

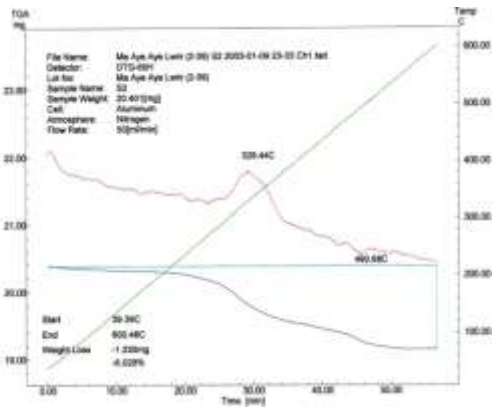

(b) BiOCl-2

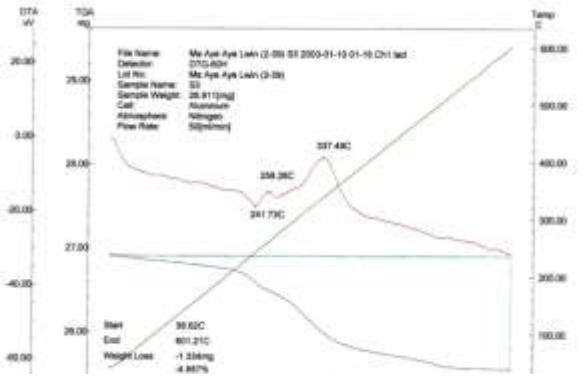

(c) BiOCl-3

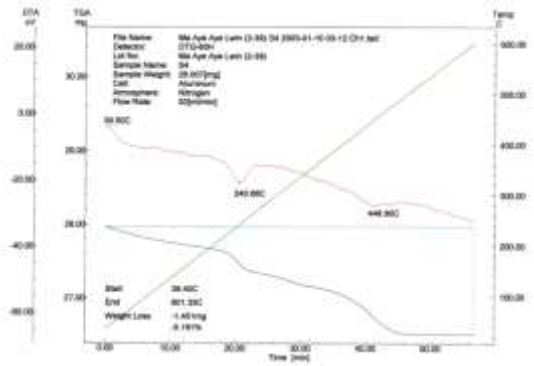

(d) BiOCl-4

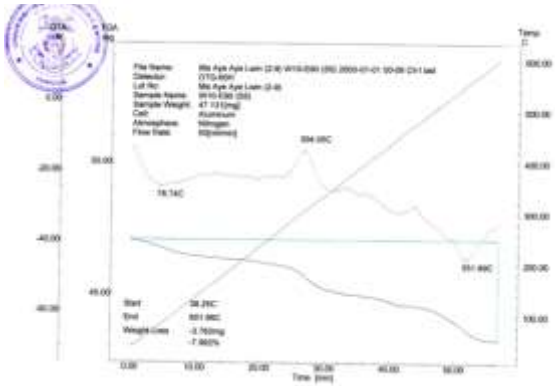

(e) BiOCl-5

Figure 6. TG -DTA thermogram of BiOCl NPs

Photocatalytic Performance of BiOCl NPs on RhB and EBT

The photocatalytic activity of the synthesized BiOCl NPs was evaluated by the estimation of RhB and EBT present in the solution after different durations of ultraviolet light exposure, which were subsequently related to the amount of dye degraded in a specific interval of time under identical exposure conditions. For synthesized samples, the photocatalytic performance was gradually enhanced as the ethanol ratio increased from 10% to 75%. Among all the samples, the concentrations of BiOCl-3 (~0.0509) and BiOCl-4 (~0.0063) showed the highest photocatalytic activity of ~0.0063 on RhB and the concentration of BiOCl-4 (~0.015) and BiOCl-5 (~0.051) showed the highest photocatalytic activity of ~0.015 on EBT. As seen in Figure 7, the catalytic efficiency can achieve ~100 % removal within 1 h on RhB and 30 min on EBT. The ethanol ratio was increased to 75 %, leading to an increase in photocatalytic degradation activity.

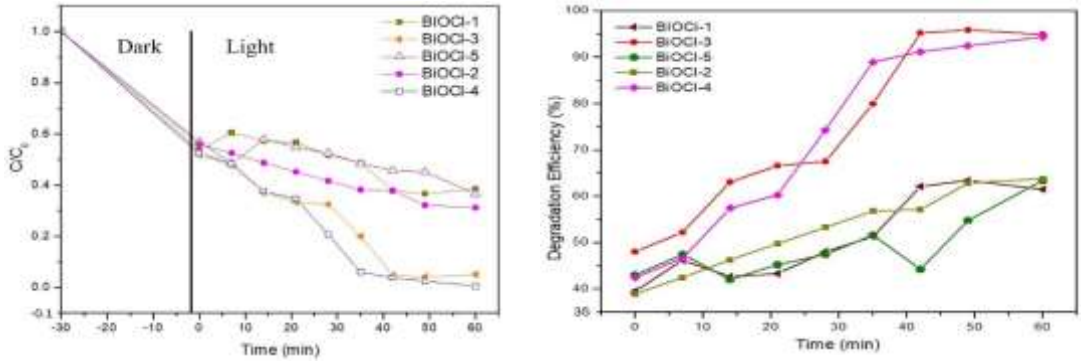

(a)

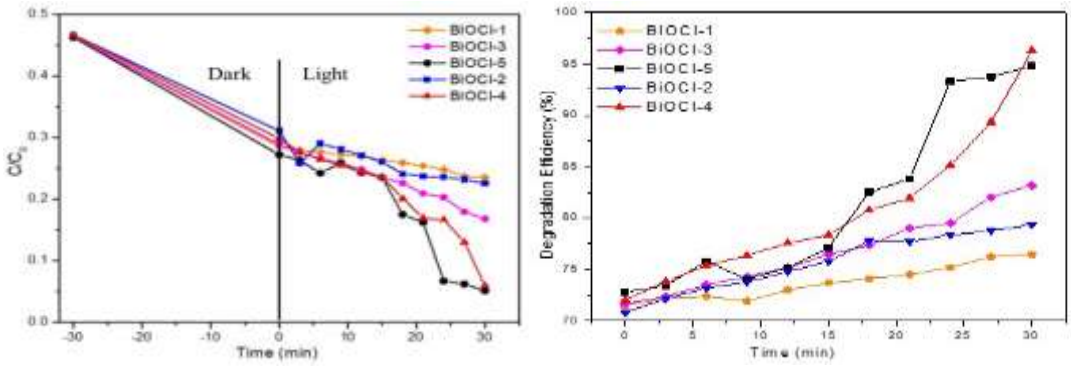

(b)

Figure 7. Comparison of photocatalytic activity and degradation efficiency of BiOCl 1 to 5 for degradation performance with (a) RhB and (b)EBT under UV light irradiation

Mechanism of Photocatalytic Activity of Synthesized BiOCl-4 NPs

The mechanism of the photocatalytic activity of BiOCl-4 can be attributed to electron and hole recombination. The conduction band (CB) and valence band (VB) for a semiconductor can be calculated according to the following theoretical empirical formulae

$$E_{CB} = \chi - E^e - 0.5E_g$$

$$E_{VB} = E_{CB} + E_g$$

where E_{CB} is the conduction band (CB) energy; χ is the absolute electronegativity of the constituent atoms, expressed as the arithmetic mean of the atomic electron affinity and the first ionization energy; E^e is the energy of free electrons on the hydrogen scale (~4.5 eV); E_g is the band gap energy of the semiconductor; E_{VB} is the valence band (VB) energy. The band gap energy value for BiOCl-4 is 3.36 eV (Table 1).

Table 1. Absolute Electronegativity, Calculated Conduction Band, Valence Band and Band Gap energy for BiOCl-4

Semiconductors	Absolute electronegativity (χ) (eV)	Calculated CB energy (eV)	Calculated VB energy (eV)	Band gap energy, E_g (eV)
BiOCl-4	6.36	0.46	3.82	3.36

When the BiOCl nanosheet is irradiated by UV light, holes in the VB will be created as the electrons in the VB get excited and jump to the CB (Dan-Iya and Soylu, 2019). The generated electrons (e^-) react with dissolved oxygen molecules in the aqueous solution to produce superoxide anion radicals ($O_2^{\bullet -}$), while the positively charged holes (h^+) can react with hydroxide anions (OH^-) derived from water to make hydroxyl radicals ($OH^\bullet$). Degradation of the RhB and EBT dye molecules to make degradation products (CO_2, H_2O) took place through their reaction with the superoxide anion and hydroxyl radicals (Figure 8). Based on the above results, a possible photocatalytic pathway for BiOCl was proposed, as outlined as below.

$$BiOCl + h\nu \rightarrow BiOCl(h^+) + BiOCl(e^-)$$
$$O_2 + e^- \rightarrow O_2^{\bullet -}$$
$$h^+ + OH^- \rightarrow OH^\bullet$$
$$h+ + H_2O \rightarrow OH^\bullet + H^+$$
$$O_2^{\bullet -} \text{ or } OH^\bullet + \text{organic dye} \rightarrow \text{degradation products}$$

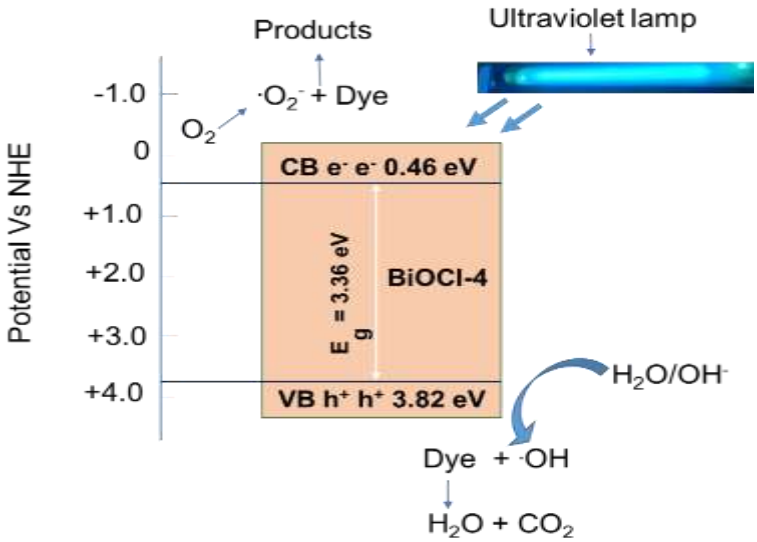

Figure 8. Schematic diagram of the photocatalytic mechanism for the dye degradation under ultraviolet light

Conclusion

Well-crystallized flake-like bismuth oxychloride (BiOCl) nanosheets were successfully synthesized by a solvothermal process. The XRD diffractogram of BiOCl NPs showed the major diffraction peaks at Miller indices of (001), (101), (110), and (012). The average crystallite sizes of BiOCl NPs obtained from the Debye-Scherrer equation were found to be in the range of 19.92 to 32.23nm. The SEM images of BiOCl NPs revealed that BiOCl-4 had the highest number of flake-like nanosheets. According to UV spectra, BiOCl NPs showed wavelengths of maximum

absorption ranging from 210-275 nm activity due to n to π* electronic transition of BiOCl NPs. FT IR spectra showed the functional groups of synthesized BiOCl NPs. TG-DTA thermogram showed the total weight loss percentages of BiOCl NPs were 3.48 to 10.30 %. BiOCl-4 showed the highest photocatalytic due to lower band gap values than other samples. These results indicated that BiOCl NPs may be suitable photocatalysts for wastewater and industrial textile wastewater treatment due to their enhanced photocatalytic activities.

Acknowledgements

The authors would like to thank Professor Dr Ni Ni Than, Head of Department of Chemistry, University of Yangon, for giving us permission to present this research paper at the Paper Reading Session organized by Myanmar Academy of Arts and Science. We would like to acknowledge Professors Dr Ye Myint Aung, Dr Myat Kyaw Thu, Dr San San Aye and Dr Nyan Tun, Department of Chemistry, University of Yangon for their valuable suggestions and advice throughout this research work. Finally, we are also thankful to, Universities' Research Center, West Yangon University and Pathein University, for providing XRD, TG-DTA, SEM, and FT IR facilities.

References

Cao, S., C. Guo, Y. Lv, Y. Guo, and Q. Liu. (2009). "A Novel BiOCl Film with Flowerlike Hierarchical Structure and Its Optical Properties". *Nanotechnology*, vol. 20, pp. 1-7

Dan-Iya, B.I., and Soylu, G.S.P. (2019). "Preparation and Characterization of Bismuth Oxychloride Nanoparticles for The Development of Photocatalytic Performance". *J. Indian Chem. Soc*., vol. 96, pp.1205-1209

Dudchenko, N, S. Pawar, I. Perelshtein, and D. Fixler. (2022). "Magnetite Nanoparticles: Synthesis and Application in Optics and Nanophotonics". *Materials*, vol. 15, pp. 1-34

Schwartz, J.C.P (Ed) (1965). *Physical Methods in Organic Chemistry*. London: Robert Cunningham and Sons, Ltd.

Seddigi, Z.S., M. A. Gondal, U. Baig, S. A. Ahmed, M.A. Abdulaziz, E. Y. Danish, M. M. Khaled, and A. Lais. (2017). "Facile Synthesis of Light Harvesting Semiconductor Bismuth Oxychloride Nano Photo-catalysts for Efficient Removal of Hazardous Organic Pollutants". *PLOS ONE*, vol.12(2), pp. 1-19

Sharma, I. D., G. K. Tripathi, V. K. Sharma, S. N. Tripathi, R. Kurchania, C. Kant, A. K. Sharma, and K. K. Saini. (2015). "One-pot Synthesis of Three Bismuth Oxyhalides (BiOCl, BiOBr, BiOl) and their Phytocatalytic Properties in Three Different Exposure Conditions". *Cogent Chemistry*, vol. 1, pp. 1-15

Silverstein, R.M., and Webster, F. X. (1998). *Spectrometric Identification of Organic Compounds*. New York: 6th edition John Wiley and Sons

Tripathi, G. K., K. K. Saini, and R. Kurchania. (2015). "Synthesis of Nanoplate Bismuth Oxychloride – A Visible Light Active Material". *Optics and Spectroscopy*, vol. 119, pp. 656-663

Wang, L., Y. Liu, G. Chen, M. Zhang, X. Yang, R. Chen, and Y. Cheng. (2022). "Bismuth Oxychloride Nanomaterials Fighting for Human Health; From Photodegradation to Biomedical Application". *Crystal*, vol. 12, pp. 1-23